PROCEEDINGS OF SCIENCE

Constraints on the $s - \bar{s}$ asymmetry of the proton in chiral effective theory

X.G. Wang*
CoEPP and CSSM, University of Adelaide, Adelaide SA 5005, Australia
E-mail: xuan-gong.wang@adelaide.edu.au

We investigate the $s - \bar{s}$ asymmetry in the proton in chiral effective theory. Unlike previous meson cloud model calculations, which accounted for kaon loop contributions with on-shell intermediate states alone, this work includes off-shell terms and contact interactions, which impact the shape of the $s - \bar{s}$ difference. We use the hyperon production data and the latest results from global PDF fits to constrain the parameters within Pauli-Villars regularization procedure, which preserves chiral symmetry and Lorentz invariance. We also extract the correction to the NuTeV anomaly from strange asymmetry effect.

The 26th International Nuclear Physics Conference
11-16 September, 2016
Adelaide, Australia

*Speaker.

© Copyright owned by the author(s) under the terms of the Creative Commons Attribution-NonCommercial-NoDerivatives 4.0 International License (CC BY-NC-ND 4.0).

PoS(INPC2016)294

1. Introduction

The nature of the quark-antiquark sea continues to challenge our understanding of the nonperturbative structure of the nucleon. In addition to the light quark sea, which has been shown to display nontrivial structure [1, 2, 3], the heavier quarks such as the strange or even the charm quark could contribute to the internal nucleon dynamics. The role played by strange quarks in the proton spin [4] and in electroweak form factors [5] has been explored extensively in the literature. Regarding to the strange quark distribution functions, most parametrizations from global fit to Deep Inelastic Scattering (DIS) data assume $s(x) = \bar{s}(x)$.

There are two mechanism that can generate asymmetric strange quark distributions in the proton. The perturbative contribution arises from gluon radiation at three-loop level [6]. Nonperturbatively, the asymmetric dissociation of the nucleon into a hyperon (containing the s quark) and a kaon (containing the $\bar{s}$ antiquark) automatically generates asymmetric distributions for the s and $\bar{s}$ PDFs.

While the existence of strange asymmetry is not surprising, the magnitude and even the sign of the asymmetry has been far more difficult to determine. Both phenomenological analysis [7] and model calculations [8] are subject to fairly large uncertainties, because of various approximations and model assumptions made about nuclear corrections and functional forms for the PDFs.

A more systematic approach with direct connection to the underlying QCD theory is needed. In recent work [9, 10], we investigated the strange and anti-strange quark distributions in the proton within chiral effective theory, which preserves chiral symmetry and gauge invariance.

2. Formalism

The $(n-1)$th spin independent (SI) Mellin moments of the quark distribution functions are defined as

$$\langle x^{n-1} \rangle_q^B = \int_0^1 dx x^{n-1} \left(q^B(x) + (-1)^n \bar{q}^B(x) \right) . \tag{2.1}$$

The operator product expansion (OPE) allows these moments to be related to the matrix elements of local twist-two quark operators $\mathscr{O}_q$ by

$$\langle N | \mathscr{O}_q^{\mu_1 \ldots \mu_n} | N \rangle = 2 \langle x^{n-1} \rangle_q p^{\{\mu_1} \ldots p^{\mu_n\}} , \tag{2.2}$$

where the operators are given by quark bilinears

$$\mathscr{O}_q^{\mu_1 \ldots \mu_n} = i^{n-1} \bar{q} \gamma^{\{\mu_1} \overleftrightarrow{D}^{\mu_2} \ldots \overleftrightarrow{D}^{\mu_n\}} q , \tag{2.3}$$

with $\overleftrightarrow{D} = \frac{1}{2} \left(\overrightarrow{D} - \overleftarrow{D} \right)$.

In an effective field theory (EFT), these quark operators are matched to hadronic operators with the same quantum numbers [11] ,

$$\mathscr{O}_q^{\mu_1 \ldots \mu_n} = \sum_{j=1}^{\infty} c_{q/j}^{(n)} \mathscr{O}_j^{\mu_1 \ldots \mu_n} , \tag{2.4}$$

where j labels different types of hadronic operators.

PoS(INPC2016)294

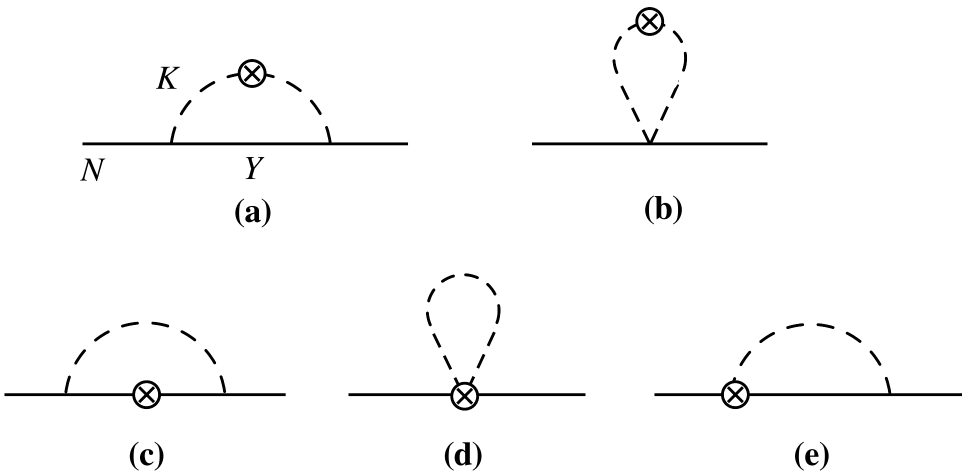

Figure 1: Contributions to $\bar{s}$ PDF in the nucleon from (a) the kaon rainbow and (b) kaon bubble diagrams, and contributions to the s PDF from (c) the hyperon rainbow, (d) kaon tadpole, and (e), (f) Kroll-Ruderman diagrams. The kaons K and hyperon Y are represented by the internal dashed and solid curves, respectively, and the crosses represent insertions of the operators in Eq. (2.5).

PoS(INPC2016)294

The local twist-two quark operators can be matched to hadronic operators [10, 12]

$$\begin{aligned}
\mathscr{O}_q^{\mu_1\cdots\mu_n} &= a^{(n)} i^n \frac{f_\phi^2}{4}\Big\{\mathrm{Tr}\left[U^\dagger \lambda_+^q \partial_{\mu_1}\cdots\partial_{\mu_n} U\right] + \mathrm{Tr}\left[U \lambda_+^q \partial_{\mu_1}\cdots\partial_{\mu_n} U^\dagger\right]\Big\} \\
&+ \left[\alpha^{(n)}(\overline{\mathscr{B}}\gamma^{\mu_1}\mathscr{B}\lambda_+^q) + \beta^{(n)}(\overline{\mathscr{B}}\gamma^{\mu_1}\lambda_+^q\mathscr{B}) + \sigma^{(n)}(\overline{\mathscr{B}}\gamma^{\mu_1}\mathscr{B})\,\mathrm{Tr}[\lambda_+^q]\right] p^{\mu_2}\cdot\cdot p^{\mu_n} \\
&+ \left[\bar{\alpha}^{(n)}(\overline{\mathscr{B}}\gamma^{\mu_1}\gamma_5\mathscr{B}\lambda_-^q) + \bar{\beta}^{(n)}(\overline{\mathscr{B}}\gamma^{\mu_1}\gamma_5\lambda_-^q\mathscr{B}) + \bar{\sigma}^{(n)}(\overline{\mathscr{B}}\gamma^{\mu_1}\gamma_5\mathscr{B})\,\mathrm{Tr}[\lambda_-^q]\right] p^{\mu_2}\cdots p^{\mu_n} \\
&+ \text{permutations} - \mathrm{Tr}\,.
\end{aligned} \tag{2.5}$$

The operators proportional to $\bar{\alpha}^{(n)}$, $\bar{\beta}^{(n)}$ and $\bar{\sigma}^{(n)}$, which are necessary to preserve the gauge invariance, will give rise to the so-called Kroll-Ruderman (KR) diagrams as shown in Fig. 1.

The loop contributions to $\bar{s}$ and s can be written as a standard convolution of hadronic splitting functions and strange quark distributions in hadronic configurations,

$$\begin{aligned}
\bar{s}(x) &= \Big(\sum_{KY} f_{KY}^{(\mathrm{rbw})} + \sum_K f_K^{(\mathrm{bub})}\Big) \otimes \bar{s}_K, \\
s(x) &= \sum_{YK}\Big(\bar{f}_{YK}^{(\mathrm{rbw})} \otimes s_Y + \bar{f}_{YK}^{(\mathrm{KR})} \otimes s_Y^{(\mathrm{KR})}\Big) + \sum_K \bar{f}_K^{(\mathrm{tad})} \otimes s_K^{(\mathrm{tad})}\,,
\end{aligned} \tag{2.6}$$

where $\bar{f}(y) = f(1-y)$, and $y = k^+/p^+$ is the kaon light-cone moment fraction.

The strange-quark hyperon PDFs, s_Y, are related to the u and d PDFs in the proton using SU(3) symmetry,

$$s_\Lambda = (2u-d)/3\,, \quad s_{\Sigma^+} = s_{\Sigma^0} = d\,, \tag{2.7}$$

while the Kroll-Ruderman distributions, $s_Y^{(\mathrm{KR})}$, are related through SU(3) symmetry to the spin-dependent PDFs in the proton,

$$s_\Lambda^{(\mathrm{KR})} = (2\Delta u - \Delta d)/(3F+D)\,, \quad s_{\Sigma^+}^{(\mathrm{KR})} = s_{\Sigma^0}^{(\mathrm{KR})} = \Delta d/(F-D)\,. \tag{2.8}$$

Taking the hyperon rainbow diagram as an example, the hadronic splitting functions can be derived by computing the nucleon matrix elements of hadronic operators,

$$f_{YK}^{(\mathrm{rbw})}(y) = \frac{C_{KY}^2 \overline{M}^2}{(4\pi f_P)^2} \left[f_Y^{(\mathrm{on})}(y) + f_Y^{(\mathrm{off})}(y) - f_K^{(\delta)}(y) \right] , \tag{2.9}$$

where $\overline{M} = M + M_Y$ and

$$\begin{aligned} f_Y^{(\mathrm{on})}(y) &= y \int dk_\perp^2 \, \frac{k_\perp^2 + [M_Y - (1-y)M]^2}{(1-y)^2 D_{KY}^2} F^{(\mathrm{on})}(y, k_\perp^2) \\ f_Y^{(\mathrm{off})}(y) &= \frac{2}{\overline{M}} \int dk_\perp^2 \, \frac{[M_Y - (1-y)M]}{(1-y) D_{KY}} F^{(\mathrm{off})}(y, k_\perp^2) \\ f_K^{(\delta)}(y) &= \frac{1}{\overline{M}^2} \int dk_\perp^2 \, \log \Omega_K \, \delta(y) \, F^{(\delta)}(y, k_\perp^2) , \end{aligned} \tag{2.10}$$

with

$$D_{KY} \equiv -\frac{1}{1-y} [k_\perp^2 + y M_Y^2 + (1-y) m_K^2 - y(1-y) M^2] \tag{2.11}$$

being the kaon virtuality for an on-shell hyperon intermediate state, and $\Omega_K = k_\perp^2 + m_K^2$.

All other splitting functions can be expressed in terms of the above three functions in Eq. (2.10). The rainbow and KR splitting functions satisfy

$$f_{KY}^{(\mathrm{rbw})} = f_{YK}^{(\mathrm{rbw})} + f_{YK}^{(\mathrm{KR})} , \tag{2.12}$$

and the tadpole contribution is related to the bubble term,

$$f_K^{(\mathrm{bub})} = f_K^{(\mathrm{tad})} . \tag{2.13}$$

These two conditions guarantee that the net strangeness in the nucleon is zero.

To regulate the ultraviolet divergence, we utilize Pauli-Villars (PV) scheme, which preserves all required symmetries. For the on-shell splitting function, one replaces the $1/D_{KY}^2$ propagator by $1/D_{KY}^2 - 1/D_{\mu_1}^2$, where $D_{\mu_1} = k^2 - \mu_1^2$. The regulating function is

$$F^{(\mathrm{on})} = 1 - \frac{D_{KY}^2}{D_{\mu_1}^2} . \tag{2.14}$$

Similarly, the off-shell regulating function can be obtained

$$F^{(\mathrm{off})} = 1 - \frac{D_{KY}}{D_{\mu_1}} . \tag{2.15}$$

To regulate the δ-function term, we need to introduce two subtraction terms to the kaon propagator,

$$\frac{1}{D_K} \to \frac{1}{D_K} - \frac{a_1}{D_{\mu_1}} - \frac{a_2}{D_{\mu_2}} , \tag{2.16}$$

where

$$a_1 = \frac{\mu_2^2 - m_K^2}{\mu_2^2 - \mu_1^2} , \;\; a_2 = -\frac{\mu_1^2 - m_K^2}{\mu_2^2 - \mu_1^2} . \tag{2.17}$$

The corresponding regulating function is

$$F^{(\delta)} = 1 - \frac{a_1 \Omega_{\mu_1} + a_2 \Omega_{\mu_2}}{\log \Omega_K} . \tag{2.18}$$

The only free parameters in the calculation are these two cutoffs μ_1 and μ_2.

PoS(INPC2016)294

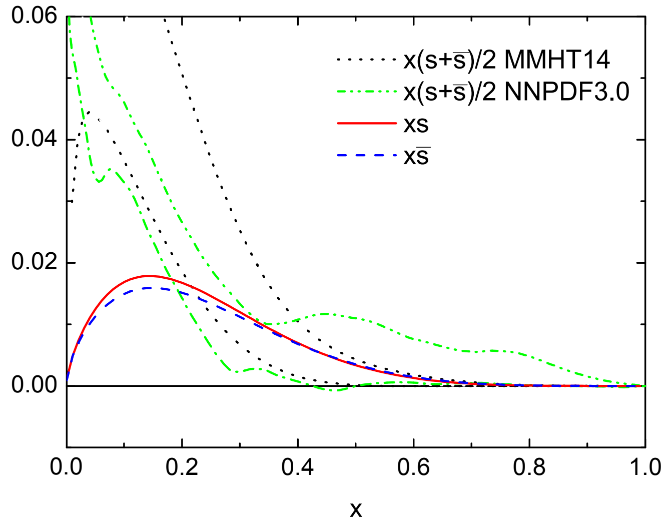

Figure 2: Comparison between the strange xs (solid red curve) and antistrange $x\bar{s}$ (dashed blue curve) PDFs from kaon loops, for the cutoff parameters ($\mu_1 = 545$ MeV and $\mu_2^{\max} = 600$ MeV), with the global fits.

3. Numerical Results

The parameter μ_1 can be determined by fitting the differential cross section data of $pp \to \Lambda X$ with one-kaon-exchange [9, 10]. The best fit value for the cutoff is $\mu_1 = 545$ MeV. As a conservative estimate of the impact of non-kaonic backgrounds, we also consider the fit that is two standard deviations lower, which corresponds to $\mu_1 = 526$ MeV.

For fixed μ_1, the allowed range for μ_2 with the PV regularization is $m_K \leq \mu_2 \leq \mu_2^{\max}$. The upper limit $\mu_2^{\max}$ can be obtained by requiring the loop contribution to $x(s+\bar{s})$ does not exceed the phenomenological parametrization at $Q^2 = 1$ GeV^2 within the quoted uncertainties, $x(s+\bar{s})_{\text{loop}} \leq x(s+\bar{s})_{\text{tot}}$, for any value of x. This is illustrated in Fig. 2, for the preferred value $\mu_1 = 545$ MeV, where the phenomenological results are taken from MMHT [13] and NNPDF [14] collaborations. Using the lower value, $\mu_1 = 526$ MeV, permits a higher upper limit, $\mu_2^{\max} = 894$ MeV, that still satisfies the constraint in Fig. 2.
Within these limits of cutoff parameters, the second moment

$$S^- = \int_0^1 x\,[s(x) - \bar{s}(x)]\,dx \tag{3.1}$$

lies in the range

$$-0.07 \times 10^{-3} \leq S^- \leq 1.12 \times 10^{-3}\ . \tag{3.2}$$

The corrections Δs_W^2 to s_W^2 arising from strange quark asymmetry is given by [15],

$$\Delta s_W^2|_{\text{strange}} = \int_0^1 F[s_W^2, s(x) - \bar{s}(x); x]x[s(x) - \bar{s}(x)]dx \tag{3.3}$$

at $Q^2 = 10$ GeV^2. Varying the μ_1 and μ_2 parameters over their maximally allowed range, we find a correction, $\Delta(\sin^2\theta_W)$, to the weak angle from the strange asymmetry of

$$-7.7 \times 10^{-4} \leq \Delta(\sin^2\theta_W) \leq -6.7 \times 10^{-7}\ . \tag{3.4}$$

PoS(INPC2016)294

This is of the right sign to reduce the discrepancy between the NuTeV value and the world average, but the magnitude is too small to account for the anomaly.

4. Conclusion

We have calculated the full set contributions to $s-\bar{s}$ asymmetry within chiral effective field theory. Both strange and anti-strange quark distributions can be expressed as a standard convolution form. Our analysis reveals new contribution to the $\bar{s}$ PDF, which is proportional to $\delta(x)$, as well as small but nonzero valence-like component of the s PDF. By taking into account the experimental data from inclusive Λ production in pp scattering and the latest results from global PDF fits, our analysis gives the most reliable estimate to date of the strange quark asymmetry. Its effect on the NuTeV anomaly is also extracted, which only reduces the NuTeV anomaly by less than 0.5 σ.

Acknowledgements

I would like to thank Chueng-Ryong Ji, W. Melnitchouk, A.W. Thomas, Y. Salamu and P. Wang for fruitful collaborations. This work was supported by the Australian Research Council through the ARC Centre of Excellence for Particle Physics at the Terascale (CE110001104), an ARC Australian Laureate Fellowship FL0992247 (AWT) and DP151103101.

References

[1] M. Arneodo *et al.*, Phys. Rev. D **50** (1994) R1.

[2] R.S. Towell *et al.*, Phys. Rev. D **64** (2001) 052002.

[3] A.W. Thomas, Phys. Lett. **126 B** (1983) 97.

[4] J. Ashman *et al.*, Nucl. Phys. B 328 (1989) 1.

[5] R.D. Young, J. Roche, R. D. Carlini and A. W. Thomas, Phys. Rev. Lett. 97 (2006) 102002.

[6] S. Catani, D. de Florian, G. Rodrigo and W. Vogelsang, Phys. Rev. Lett. **93**, 152003 (2004).

[7] W. Benz, I.C. Cloët, J.T. Londergan and A.W. Thomas, Phys. Lett. B 693 (2010) 462.

[8] T.J. Hobbs, M. Alberg and G. A. Miller, Phys. Rev. C 91 (2015) 035205.

[9] X.G. Wang, C.-R. Ji, W. Melnitchouk, Y. Salamu, A. W. Thomas and P. Wang, Phys. Lett. B **762** (2016) 52.

[10] X.G. Wang, C.-R. Ji, W. Melnitchouk, Y. Salamu, A. W. Thomas and P. Wang, Phys. Rev. D **94** (2016) 094035.

[11] J.-W. Chen and X. Ji, Phys. Rev. Lett. **87**, 152002 (2001); **88**, 249901(E) (2002).

[12] P.E. Shanahan, A.W. Thomas and R.D. Young, Phys. Rev. D **87** (2013) 114515.

[13] L. A. Harland-Lang, A. D. Martin, P. Motylinski and R. S. Thorne, Eur. Phys. J. C **75**, 204 (2015).

[14] R. D. Ball *et al.*, JHEP **04** (2015) 040.

[15] G. P. Zeller *et al.*, Phys. Rev. D **65** (2002) 111103(R).

PoS(INPC2016)294